1279. Experimental investigation of the vibration transmissibility of a magnet-spring vibration isolator under random excitation

Kihong Shin
Department of Mechanical & Automotive Engineering, Andong National University
Andong, 760-749, Korea
E-mail: *kshin@anu.ac.kr*

(Received 20 October 2013; received in revised form 14 December 2013; accepted 21 December 2013)

Abstract. A magnet-spring vibration isolator comprised of several magnets and mechanical springs has been proved to be highly effective for overcoming the major limitation of a conventional linear vibration isolator in such a way that the stiffness of the isolator is sufficiently large to hold the weight of a load, but becomes much softer under dynamic motion. The vibration transmissibility of this magnet-spring vibration isolator is usually examined using a sinusoidal excitation with a specific frequency because the system is nonlinear. In this paper, the isolation performance of the magnet-spring vibration isolator is further investigated experimentally for the case of random base excitation. The experimental results are compared with the cases of sinusoidal excitation obtained by computer simulations considering both jump-up and jump-down transmissibility curves. The results are interesting: the vibration isolation performance improves as the RMS (Root Mean Square) amplitude of the random base excitation increases; the experimental vibration transmissibility curve of the random excitation is bounded by the jump-up transmissibility curve of the corresponding sinusoidal excitation case.

Keywords: vibration isolation, magnet-spring, high-static-low-dynamic stiffness (HSLDS), negative stiffness, nonlinear, random excitation.

Nomenclature

A_{rms}	root mean square of the excitation amplitude of the shaker base
L	length between attracting magnets
m	mass
c	damping
k	stiffness
x	displacement of the mass
u	displacement of the base
F_m	net magnetic force
f_m	mass normalized net magnetic force
ω	excitation frequency
ω_n	natural frequency of a linear system
ω_m	equivalent natural frequency without linear springs
ζ	damping ratio

1. Introduction

Vibration isolation is one of the most important and frequently encountered practical engineering applications in machinery industry. Whether the vibration of a machine is controlled not to be transmitted to neighboring structures or the external vibration is controlled not to be transferred to the machine, a typical method is to install a linear vibration isolator having an appropriate stiffness. The linear vibration isolator has a limited performance such that the isolation frequency region is $\omega > \sqrt{2}\omega_n$, where ω_n is the natural frequency defined by the isolator's stiffness and the mass of the payload. This frequency limited performance cannot be improved by

using a softer isolator since the stiffness of the isolator must be high enough to hold the payload adequately. This is known as the fundamental constraint of a linear vibration isolator.

While several ideas have been suggested to improve the isolation performance by using nonlinear magnetic forces [1-7], a mechanism consisted of permanent magnets and linear springs has been proved to be highly effective for alleviating the fundamental limitation of a linear vibration isolator by achieving the characteristic of high-static-low-dynamic stiffness (HSLDS) [5, 8, 9]. This magnet-spring vibration isolator behaves softly when it responds to a dynamic motion, while it has a high enough static stiffness to accommodate the payload.

The principle of the magnet-spring vibration isolator was introduced by Carrella et al. [5]. Since then, Shin has verified its practical usability by extensive experiments taking into account of a suggested key system parameter and the amplitude dependent nonlinearity of the system [9]. Their results however were obtained based on the sinusoidal base excitation only, and thus it may not be fully validated for real engineering application especially where the excitation nature is random like.

In this paper, the magnet-spring vibration isolator is further examined for the case of random base excitation. Since the magnet-spring vibration isolator is highly nonlinear, the analytic description of the response to random excitation cannot be easily obtained. Further, the author has found that the numerical simulation is not feasible due to large numerical errors produced during the numerical integration process of solving the mathematical model of the magnet-spring vibration isolator, especially when the amplitude of random excitation is large. Thus, in this paper, the vibration transmissibility of the magnet-spring vibration isolator is investigated by experiments for various values of the system parameter and for different levels of random excitation. In order to understand the dynamics more clearly, the experimental results of random excitation are compared with the cases of sinusoidal excitation obtained by computer simulations with carefully selected values of parameters. In the following section, the vibration transmissibility of the magnet-spring vibration isolator is examined by computer simulation with consideration of the jump-up and jump-down frequencies. Then, experimental results of random excitation are presented in section 3, by considering both the key system parameter and the excitation level. Finally, concluding remarks are given.

2. The jump-up and jump-down transmissibility curves of the magnet-spring vibration isolator

In this section, the theoretical model of the magnet-spring vibration isolator is briefly given with a key system parameter. Then, typical jump-up and jump-down transmissibility curves under sinusoidal base excitation are examined by computer simulation.

Consider the theoretical model of the magnet-spring vibration isolator as shown in Figure 1, where both the upper and lower pairs of magnets are configured to attract each other, and the linear springs between magnets prevents the system becoming unstable, i.e., the maximum repelling spring force is greater than the attracting magnetic force (F_{m1} or F_{m2}).

Normalizing the net magnetic force acting on the equipment (payload) with respect to the mass of payload, it is shown that the equation of motion and the net magnetic force can be written as [8]:

$$\ddot{x} + 2\zeta\omega_n\dot{x} + \omega_n^2 x - f_m = 2\zeta\omega_n\dot{u} + \omega_n^2 u, \tag{1}$$

$$f_m = \frac{F_m}{m} = \frac{(F_{m1} - F_{m2})}{m} = \frac{\omega_m^2 L^4 x_r}{(L^2 - x_r^2)^2}, \tag{2}$$

where $\omega_n = \sqrt{k/m}$, $\zeta = c/2m\omega_n$ and $x_r = x - u$, and ω_m is the equivalent natural frequency if only the stiffness due to the magnets is accounted for and evaluated at a neutral point.

Note that the net magnetic force introduces negative stiffness that makes the system softer under dynamic motion. The key system parameter was suggested by Shin [8] as below:

$$\alpha = \frac{\omega_m}{\omega_n}. \tag{3}$$

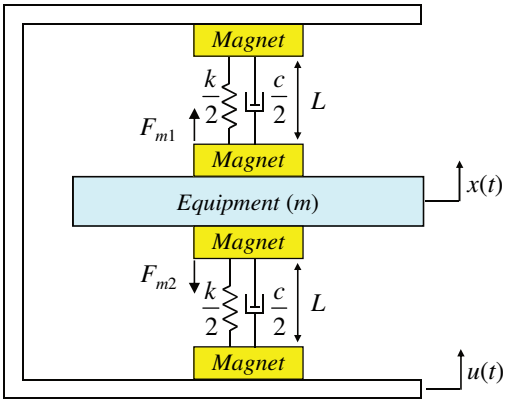

Fig. 1. Theoretical model of the magnet-spring vibration isolator

This system parameter can be used as the measure of vibration isolation improvement with respect to the isolation performance of the corresponding linear vibration isolator. Vibration transmissibility curves for various values of α have been investigated by computer simulations and experiments [8, 9]. It must be noted, however, that these curves are corresponding to the jump-down transmissibility curve, because only the maximum transmissibility was concerned in these references.

For computer simulations, $\zeta = 0.01$ and $\omega_n = 78$ rad/s (12.42 Hz) are fixed, and different values of ω_m corresponding to pre-defined lengths L are used as shown in Table 1. These values are carefully chosen from previous experimental results [9], and are directly related to the experiments shown in the next section. Also, two different levels of harmonic base excitation, $u(t) = \sqrt{2}A_{\text{rms}} \cos \omega t$, are considered such that the root mean square (RMS) values are $A_{\text{rms}} = 0.4$ mm and $A_{\text{rms}} = 0.8$ mm respectively. The use of the RMS value may be more sensible to relate the simulation results with the experimental results of random base excitation.

Table 1. Parameters for computer simulations

Length (L)	Equivalent natural frequency (ω_m)	System parameter (α)
52 mm	36.4 rad/s (5.8 Hz)	0.47
47 mm	41.5 rad/s (6.6 Hz)	0.53
42 mm	47.8 rad/s (7.6 Hz)	0.61

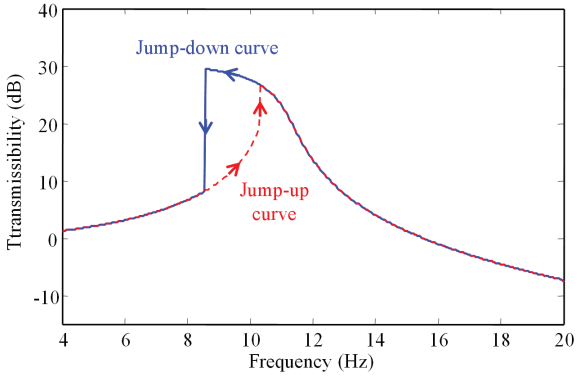

Fig. 2. An example of the jump-up and jump-down transmissibility curves (for $\alpha = 0.47$ and $A_{rms} = 0.8$ mm)

The jump-up transmissibility curve is obtained by plotting each steady state transmissibility for each given excitation frequency, as the excitation frequency increases gradually from 4 Hz to 20 Hz. On the other hand, the jump-down transmissibility curve is obtained as the excitation frequency decreases gradually from 20 Hz to 4 Hz. For each system parameter α and excitation level, the jump-up and jump-down transmissibility curves are produced for example as shown in Figure 2.

The complete transmissibility curves for each case are shown in the next section together with the corresponding experimental results of random excitation for comparison. It is noted that in Figure 2, the maximum value of transmissibility is on the jump-down curve rather than the jump-up curve because of the softening stiffness effect.

3. Experiments

3.1. Description of the experimental set-up

The experimental model of a magnet-spring vibration isolator is shown in Figure 3, and the overall experimental set-up is shown in Figure 4. As described in the previous experiments [9], where the same devices has been used, the upper and lower magnets are fixed to an aluminum shaft that is firmly attached to the shaker head so that they move together with the shaker. The central mass of 52 g is free to move and consists of two magnets producing attracting magnetic forces with regard to the upper and the lower magnets respectively.

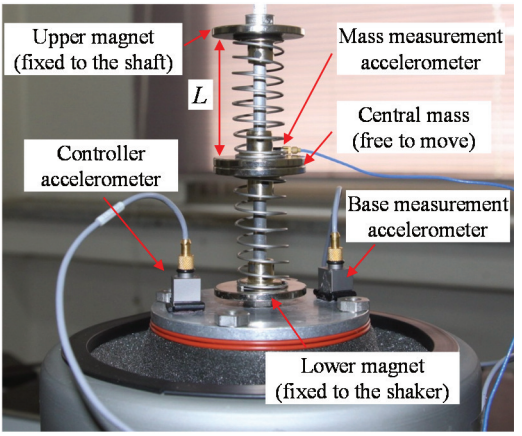

Fig. 3. Experimental model of the magnet-spring vibration isolator

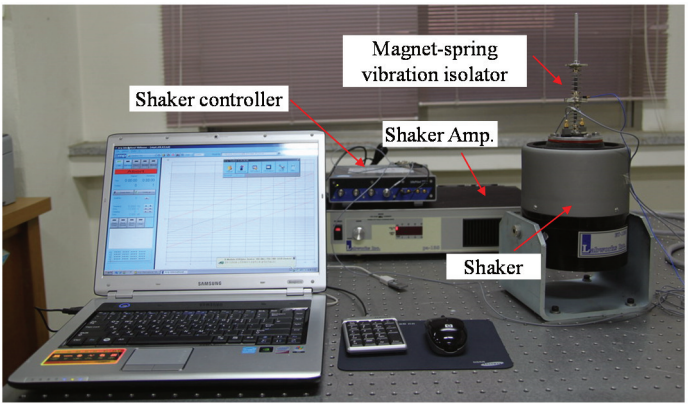

Fig. 4. Experimental set-up for the vibration transmissibility measurement

Three accelerometers are used in the experiments: the controller accelerometer for controlling the shaker movement, the base measurement accelerometer for the base vibration (i.e., the vibration of the shaker head), and the mass measurement accelerometer for measuring the vibration of the central mass.

For the experiments, three different magnetic forces are considered by adjusting the distance between the upper and the lower magnets such that the length between a pair of magnets is approximately $L = 52$ mm, 47 mm, and 42 mm. These are the same configuration used for computer simulations in the previous section, and are corresponding to the system parameter $\alpha = 0.47$, $\alpha = 0.53$, and $\alpha = 0.61$, respectively.

Gaussian random signal with a frequency band of 4 Hz to 20 Hz is generated by the shaker controller. The shaker controller also controls the excitation level of the shaker amplitude. As in the computer simulations, two levels of the shaker amplitude are considered for the experiments – a small excitation level whose RMS value is $A_{rms} = 0.4$, and a large excitation level with $A_{rms} = 0.8$ mm. The maximum amplitude of the shaker is also controlled not exceeding $\pm 3A_{rms}$.

3.2. Experimental results of the random base excitation

The vibration transmissibility curve is obtained for various values of the system parameter α and for each excitation level A_{rms} by estimating the frequency response function between the base vibration and the central mass vibration. Details of experimental results are shown in Figure 5-9.

Figure 5(a) shows the vibration transmissibility curve of random base excitation (red color) in the case of $\alpha = 0.47$ ($L = 52$ mm) and $A_{rms} = 0.4$ mm, and Figure 5(b) shows the same case but for the excitation level of $A_{rms} = 0.8$ mm. The corresponding jump-up and jump-down transmissibility curves (blue color) obtained by computer simulation are also shown for comparison.

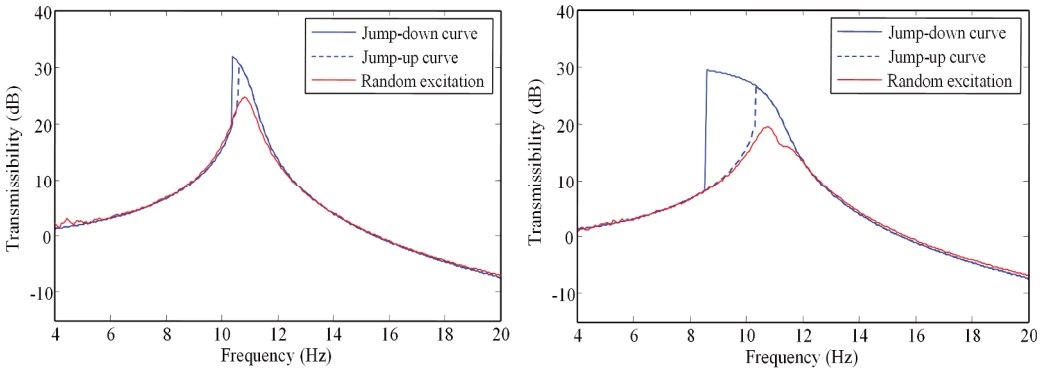

Fig. 5. Vibration transmissibility curves for $\alpha = 0.47$ ($L = 52$ mm): a) $A_{rms} = 0.4$ mm, and b) $A_{rms} = 0.8$ mm

As shown in Figure 5, the experimental vibration transmissibility curve for random excitation is very close to that for sinusoidal excitation obtained by computer simulation in the regions of low and high frequencies. However, the maximum vibration transmissibility near the resonance in the case of random excitation is much lower than that in the case of corresponding sinusoidal excitation.

It is also interesting to observe that the random vibration transmissibility curve is bounded by the jump-up sinusoidal vibration transmissibility curve rather than the jump-down transmissibility curve. In other words, for the regions of multiple (upper and lower) equilibriums, the vibration isolation performance of the magnet-spring vibration isolator under random excitation may be largely determined by the lower equilibrium. Thus, it may be concluded that the overall vibration

isolation performance of the random excitation is better than that of the sinusoidal excitation.

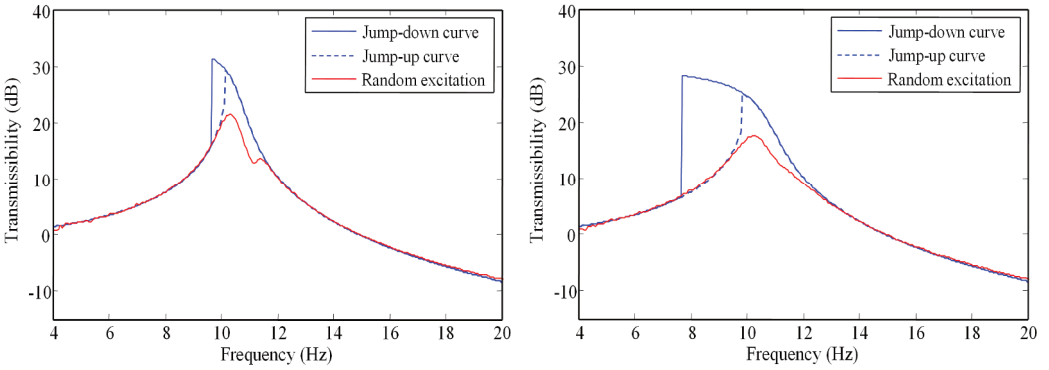

Fig. 6. Vibration transmissibility curves for $\alpha = 0.53$ ($L = 47$ mm):
a) $A_{rms} = 0.4$ mm, and b) $A_{rms} = 0.8$ mm

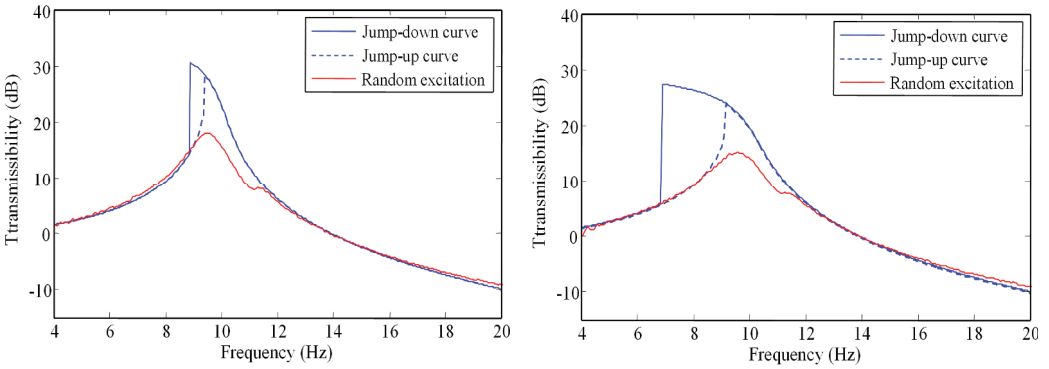

Fig. 7. Vibration transmissibility curves for $\alpha = 0.61$ ($L = 42$ mm):
a) $A_{rms} = 0.4$ mm, and b) $A_{rms} = 0.8$ mm

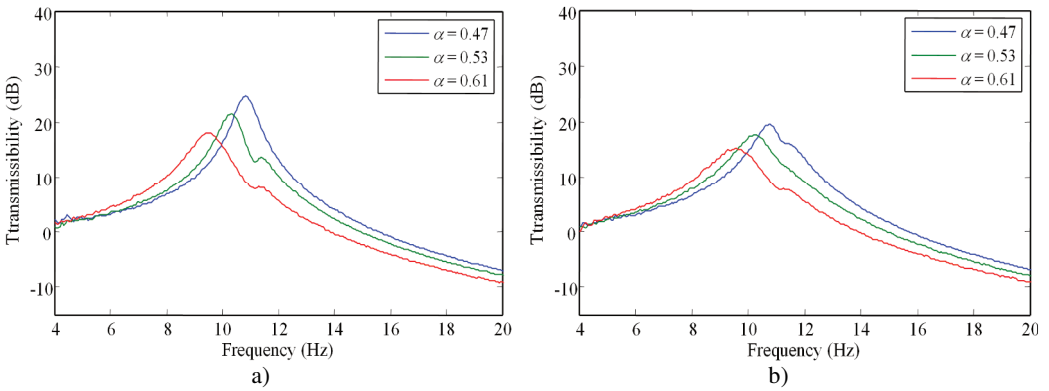

Fig. 8. Comparison of vibration transmissibility curves for various values of α:
a) $A_{rms} = 0.4$ mm, and b) $A_{rms} = 0.8$ mm

Similar experimental results are obtained for other cases: Figure 6 for $\alpha = 0.53$ ($L = 47$ mm), and Figure 7 for $\alpha = 0.61$ ($L = 42$ mm). That is, while the experimental random vibration transmissibility curves are similar to the numerically obtained sinusoidal vibration transmissibility in the regions of single equilibrium, the maximum vibration transmissibility in the case of random

base excitation is much lower than that of corresponding sinusoidal excitation.

Another observation from the experimental results is that the vibration isolation performance under random base excitation improves as the system parameter α increases as shown in Figure 8 and Figure 9. This phenomenon is the same as the case of sinusoidal excitation [9]. It is also the same as in the case of sinusoidal excitation that the vibration isolation performance of the random excitation becomes better for a larger excitation level as shown in Figure 9. Thus, it may be concluded that the system parameter α is the key factor of designing a magnet-spring vibration isolator for both sinusoidal and random base excitations.

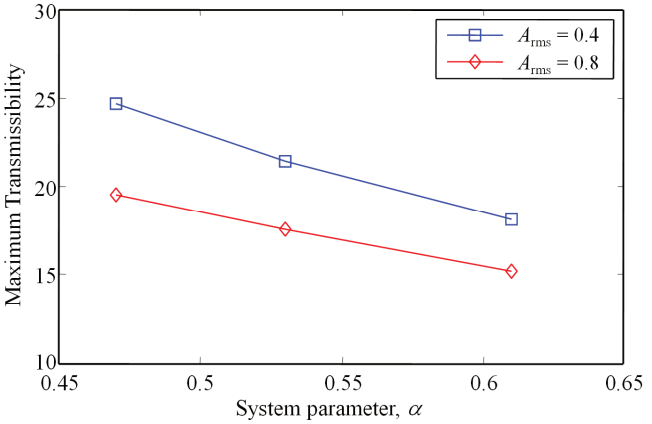

Fig. 9. Maximum vibration transmissibility with respect to the system parameter, α

4. Conclusions

In this paper, the vibration isolation performance of the HSLDS magnet-spring vibration isolator is investigated experimentally for random base excitation. The experimental results are then interpreted with the aid of simulation results of sinusoidal base excitation, by comparing with the jump-up and the jump-down transmissibility curves obtained for various values of the system parameter α with different excitation amplitudes.

Similar to the results of sinusoidal base excitation [9], the vibration isolation performance of the random excitation also improves as the system parameter α increases, and as the RMS amplitude of the base excitation increases. A few interesting properties are further observed: while the vibration transmissibility curve for random excitation is very close to that for sinusoidal excitation in the regions of low and high frequencies; the maximum vibration transmissibility near the resonance is much lower in the case of random excitation than that in the case of corresponding sinusoidal excitation, and is bounded by the jump-up transmissibility curve (i.e., the lower amplitude). Consequently, it is found that the overall vibration isolation performance of the random excitation is better than the case of sinusoidal excitation.

For the random base excitation, although the reason of the apparent lower vibration transmissibility in the resonance region cannot be explained analytically, it may be assumed that irregularly changing excitations prohibit the system settles in either upper or lower amplitude of the steady state response. This, in turn, makes the system not to have a sharp resonant characteristic but results in a highly damped characteristic especially for large amplitude.

Acknowledgement

The author would like to thank Daejoo Machinery Co. Ltd., Daegu, Republic of Korea, for continuously supporting this research. This research was originally supported by the National Research Foundation of Korea (NRF) grant funded by the Korea government (MEST) (No. 2010-0008348).

References

[1] **Puppin E., Fratello V.** Vibration isolation with magnet springs. Review of Scientific Instruments, Vol. 73, Issue 11, 2002, p. 4034-4036.

[2] **D'Angola A., Carbone G., Mangialardi L., Serio C.** Nonlinear oscillations in a passive magnetic suspension. International Journal of Non-Linear Mechanics, Vol. 41, Issue 9, 2006, p. 1039-1049.

[3] **Bonisoli E., Vigliani A.** Identification techniques applied to a passive elasto-magentic suspension. Mechanical Systems and Signal Processing, Vol. 21, Issue 3, 2007, p. 1479-1488.

[4] **Mizuno T., Takasaki M., Kishita D., Hirakawa K.** Vibration isolation system combining zero-power magnetic suspension with springs. Control Engineering Practice, Vol. 15, Issue 2, 2007, p. 187-196.

[5] **Carrella A., Brennan M. J., Waters T. P., Shin K.** On the design of a high-static-low-dynamic stiffness isolator using linear mechanical springs and magnets. Journal of Sound and Vibration, Vol. 315, Issue 3, 2008, p. 712-720.

[6] **Robertson W. S., Kidner M. R. F., Cazzolato B. S., Zander A. C.** Theoretical design parameter for a quasi-zero magnetic spring for vibration isolation. Journal of Sound and Vibration, Vol. 326, Issues 1-2, 2009, p. 88-103.

[7] **Zhou N., Liu K.** A tunable high-static-low-dynamic stiffness vibration isolator. Journal of Sound and Vibration, Vol. 329, Issue 9, 2010, p. 1254-1273.

[8] **Shin K.** Design parameter study on the isolation performance of the HSLDS magnetic vibration isolator. Transactions of the KSNVE, Vol. 20, Issue 1, 2010, p. 92-97.

[9] **Shin K.** On the performance of a single degree-of-freedom high-static-low-dynamic stiffness magnetic vibration isolator. International Journal of Precision Engineering and Manufacturing, Vol. 15, Issue 3, 2014, p. 439-445.